



# CHALMERS

## Chalmers Publication Library

### **Calculation of sound reduction by a screen in a turbulent atmosphere using the parabolic equation method**

This document has been downloaded from Chalmers Publication Library (CPL). It is the author's version of a work that was accepted for publication in:

**Acustica (ISSN: 0001-7884)**

Citation for the published paper:

Forssén, J. (1998) "Calculation of sound reduction by a screen in a turbulent atmosphere using the parabolic equation method". *Acustica*, vol. 84(4), pp. 599-606.

Downloaded from: <http://publications.lib.chalmers.se/publication/23195>

Notice: Changes introduced as a result of publishing processes such as copy-editing and formatting may not be reflected in this document. For a definitive version of this work, please refer to the published source. Please note that access to the published version might require a subscription.

Chalmers Publication Library (CPL) offers the possibility of retrieving research publications produced at Chalmers University of Technology. It covers all types of publications: articles, dissertations, licentiate theses, masters theses, conference papers, reports etc. Since 2006 it is the official tool for Chalmers official publication statistics. To ensure that Chalmers research results are disseminated as widely as possible, an Open Access Policy has been adopted. The CPL service is administrated and maintained by Chalmers Library.

(article starts on next page)

# Calculation of Sound Reduction by a Screen in a Turbulent Atmosphere Using the Parabolic Equation Method

## Abstract

Results from applying a Crank-Nicholson parabolic equation method (CN-PE) are presented in situations with a thin screen on a hard ground in a turbulent atmosphere, and with the acoustic source at ground level. The results are evaluated by comparison with G. A. Daigle's model, which uses the sound scattering cross-section by V. I. Tatarskii together with diffraction theory. The results show a fairly good agreement for situations where the receiver is above ground, thus indicating that both methods are applicable to the problem. When the receiver is at ground level the two methods lead to large differences in insertion loss since only the PE method predicts that turbulence causes an increased sound level in the case without a screen. For the situations considered in this paper a turbulent atmosphere is shown to significantly decrease the sound reduction by a screen. An approximation in the representation of a turbulent atmosphere in the CN-PE method is presented, and is shown to lead to an acceptable error in limited cases.

## 1. Introduction

In a turbulent atmosphere acoustic properties will vary stochastically from point to point giving rise to a scattered sound field that increases the sound in the acoustic shadow of a barrier. In this paper the application of the parabolic equation method (PE) to a thin screen in a turbulent atmosphere is presented, thereby further widening its applicability. In order to evaluate the results from the PE an alternative model is used, which is based on a model by Daigle [1], using the sound scattering cross-section [2] and diffraction theory.

In order to increase the understanding of how a turbulent atmosphere influences sound propagation, and to enable a better prediction of noise levels in defined realistic situations, several different models have been applied, leading to different numerical methods: the different PE methods [3, 4], the fast field program (FFP) [5], and the Heuristic model by L'Espérance *et al.* [6]

The PE method was first developed to study the propagation of radio waves in the troposphere in the mid 1940's. For sound propagation in the atmosphere a finite difference implementation of the PE was made in 1989 by Gilbert and White [7], preceded by application to underwater sound propagation. More recently a faster implementation called FAST-PE or Green's function PE (GF-PE) was implemented for outdoor sound propagation [4]. The PE method has been evaluated by comparison to other methods (e.g. [8]) and has proved to be a useful tool for a large variety of outdoor conditions: ground impedance variations [9], sound reduction by screens [10], smoothly varying terrain profiles [11], and height dependent sound speed profiles and atmospheric turbulence [3, 12]. One limitation of the PE method is that a correct solution is obtained only at low angles from the horizontal, thereby restricting the method to situations where all parts of the medium and the ground of importance to the sound field must be at low angles from the source and receiver. For instance a noise barrier must be low compared to its distance from the source and receiver.

In an upward refracting atmosphere, taking into account the effects of atmospheric turbulence is essential for predicting the sound energy in the refractive shadow zone. Turbulence causes scattering of energy into a refractive shadow and the same phenomenon occurs for the geometric shadow caused using a screen [1].

With the intention to isolate the problem with screens and turbulence the investigations of this paper are made for a hard ground. A 10 or 20 meter high screen is placed 100 or 200 meters from the source and the sound field is solved up to 1000 meters in range. It can be shown (section 2.2) that the contribution from turbulence scattering will increase relative to free field when the height of the screen, as well as its distance from source and receiver, are enlarged by the same factor. Therefore, and because of the limited angle of correct solution in the PE, these large geometries with comparably low screens are chosen. The scattering by turbulence is very small at low frequencies and therefore the calculations are made for 500 and 1000 Hz, where significant scattering occurs for these geometries. The model by Daigle using the scattering cross-section was developed for source and receiver on the ground surface, and showed reasonable agreement with measurements. In this study an additional receiver position at the height of the screen edge is used.

In section 2 of this paper the theories of the Crank-Nicholson PE method (CN-PE) and the sound scattering cross-section are briefly presented. Evaluation and comparison of the results calculated according to the two models are presented in section 3. Conclusions are in section 4. A more detailed and exten-

sive description of the CN-PE than will be given here can be found in the thesis by Galindo Arranz [9].

## 2. Theory

In order to evaluate the results of applying the PE method to a turbulent atmosphere with a screen, reference calculations are made following a similar procedure to Daigle's [1]: The energy scattered by turbulence is calculated using the sound scattering cross-section by Tatarskii [2] and is added to the diffracted energy in the shadow of the screen. In this paper the uniform theory of diffraction (UTD) [13, 14] is used to calculate the field diffracted by a thin, hard screen with the edge normal to a line through the source and receiver. For the situations considered in this paper the screen is located many wavelengths from the source and receiver, and thereby the high frequency restriction of the UTD is well fulfilled [15].

### 2.1. The Crank-Nicholson parabolic equation method

#### 2.1.1. The finite difference scheme

The PE method solves the Helmholtz equation in the far field and near the ground for the outgoing wave. The back-scattered field is neglected and the solution is obtained by an algorithm stepping forward in range an initial starting field. The parabolic equation is derived from the Helmholtz equation. In the two-dimensional case, an azimuthally independent geometry is often assumed and cylindrical co-ordinates are used. A substitution for the pressure  $p(r, z)$  is applied:

$$p(r, z) = \frac{1}{\sqrt{r}} \phi(r, z) e^{ik_0 r}, \quad (1)$$

where  $r$  is the horizontal distance from the source,  $z$  the height,  $k_0$  a reference wave number (e.g. the mean acoustic wave number in the domain of interest), and where the time factor  $\exp(-i\omega t)$  has been suppressed. The function  $\phi(r, z)$ , which is solved for in the numerical calculations, is assumed to vary more slowly in range than  $p(r, z)$ . By also applying the approximation for the far field, the two-dimensional one-way parabolic equation for the outgoing wave can be written

$$\frac{\partial \phi}{\partial r} = ik_0 \left( \sqrt{n^2 + \frac{1}{k_0^2} \frac{\partial^2}{\partial z^2}} - 1 \right) \phi, \quad (2)$$

where  $n(r, z)$  is the spatially varying index of refraction. Following Gilbert *et al.* [3] the index of refraction is written as a deterministic part  $n_d(z)$ , describing a height dependent sound speed profile, plus a range and height dependent fluctuating stochastic part  $\mu(r, z)$  describing the effect of atmospheric turbulence according to the so-called frozen turbulence hypothesis. The deterministic and stochastic parts of the index of refraction are then separated using the approximation

$$\sqrt{(n_d + \mu)^2 + \frac{1}{k_0^2} \frac{\partial^2}{\partial z^2}} \cong \sqrt{n_d^2 + \frac{1}{k_0^2} \frac{\partial^2}{\partial z^2}} + n_d \mu, \quad (3)$$

which, according to Gilbert *et al.* [3], is valid for low angles of propagation with respect to the horizontal ( $\leq 10^\circ$ ) and small fluctuations in  $\mu$  compared to the mean index of refraction ( $\leq 10^{-3}$ ).

The CN-PE uses a finite difference scheme where a system of equations with sparse matrices are preferable. Therefore the square root on the right hand side of equation (3) is approximated with a ratio of polynomials, determining the angle dependence of the error in the solution. Letting  $q = n_d^2 + k_0^{-2} \partial^2 / \partial z^2 - 1$ , and using a Padé (1, 1) approximant [16] leads to  $\sqrt{1+q} \cong (1 + \frac{3}{4}q) / (1 + \frac{1}{4}q)$ . The parabolic equation (1), can now be rewritten as

$$\left(1 + \frac{1}{4}q\right) \frac{\partial \phi}{\partial r} = ik_0 \left[\frac{1}{2}q + \left(1 + \frac{1}{4}q\right)n_d \mu\right] \phi, \quad (4)$$

after multiplication from the left by  $1 + \frac{1}{4}q$ .

Discretizing  $\partial^2 / \partial z^2 \phi(r, z)$  as  $(\phi(r, z + \Delta z) - 2\phi(r, z) + \phi(r, z - \Delta z)) / (\Delta z)^2$  and  $\partial / \partial r \phi(r, z)$  as  $(\phi(r + \Delta r, z) - 2\phi(r, z)) / (\Delta r)$ , where  $\Delta z$  and  $\Delta r$  are the size of a step in height and range respectively, the Crank-Nicholson formulation of equation (4) can be written as a system of equations with tridiagonal matrices,

$$\left(M^- - \frac{1}{2}M_\mu\right) \bar{\phi}(r + \Delta r) = \left(M^+ + \frac{1}{2}M_\mu\right) \bar{\phi}(r), \quad (5)$$

where  $\bar{\phi}$  is a column vector at a discrete range  $r$  containing elements  $\phi(r, z)$  for all discretized values of  $z$ . The matrices in equation (5) can be formally written as

$$\begin{aligned} M^\pm &= 1 + \frac{1}{4} \left(1 \pm ik_0 \Delta r\right) q, \\ M_\mu &= ik_0 \Delta r \left(1 + \frac{1}{4}q\right) n_d \mu. \end{aligned} \quad (6)$$

As starting field at  $r = 0$  a Gaussian image source is used, approximating a monopole source and its reflection at ground [4]. Other possible starting fields have been presented and tested by Galindo [9]. These alternatives can provide

a correct solution within a wider angle than the Gaussian image source. However, they only improve the solution for free propagation from the source and not for the scattering from obstacles, such as screens or turbulence.

The ground is described as an impedance plane and a second-order accurate ground boundary condition is used, as presented by West *et al.* [17].

To prevent the upper boundary of the calculation domain from causing reflections, an attenuating stratum is created by adding an imaginary part  $a(z)$  to the square of the index of refraction  $n_d$ . Following Galindo [9], the function  $a(z)$  inside the attenuating stratum can be written

$$a(z) = \left( \frac{z - z_d}{h_d} \right)^2 \exp \left( -4 \left( \frac{z - z_d - h_d}{h_d} \right)^2 \right), \quad (7)$$

where  $h_d$  is the thickness of the stratum that starts at  $z_d$ .

A thin screen is represented by setting the pressure field equal to zero from the ground and up to the screen edge at the range step of the screen. This is not a physically correct procedure, as already discussed by Salomons [10], but works for screens that are low in comparison to its distance from the source and receiver. In such cases the reflective properties of the screen are of small importance [18]; moreover, the PE can accurately predict the part of the incident field above the screen which predominantly determines the diffracted field at the receiver. The reflected wave caused by the screen is neglected, which also leads to an incorrect solution near the screen, on the receiver's side. This will only weakly affect the predictions of the turbulence scattering because both the scattering angles and the distance to the relevant receiver positions are large.

### 2.1.2. Description of turbulence

The stochastic part of the index of refraction  $\mu$  is calculated according to Gilbert *et al.* [3], assuming homogeneous and isotropic turbulence and using a Gaussian auto correlation function for  $\mu$ :

$$C_\mu(s) = \langle \mu(\mathbf{R} + \mathbf{s}) \mu(\mathbf{R}) \rangle = \mu_0^2 e^{-s^2/l^2}, \quad (8)$$

where  $\mathbf{R}$  and  $\mathbf{s}$  are two vectors in space,  $s = |\mathbf{s}|$ ,  $\mu_0$  the standard deviation of  $\mu(r, z)$ , and  $l$  the correlation length. This corresponds to a spectral density of  $\mu$  that also is Gaussian:

$$C_\mu(s) = \frac{\mu_0^2 l^2}{4\pi} e^{-\kappa^2 l^2/4}. \quad (9)$$

The representation of the turbulence in the PE method is only two-dimensional, i.e. the inhomogeneities are azimuthally constant.

The Gaussian spectral density of the fluctuating index of refraction (9) is not a physically correct description of the turbulence for the whole wave number range. However, according to [19] it can be used as an acceptable approximation in the range of wave numbers dominating the scattering in typical situations with a refractive shadow. It is assumed to be an acceptable approximation for the situations considered here as well.

A turbulent atmosphere varies over time as well as in space and therefore the PE is applied to many different realisations of  $\mu(r, z)$ , seen as instantaneous representations of a turbulent atmosphere, each fulfilling the Gaussian auto correlation function (8). In this way mean value and standard deviation of the acoustic energy at a receiver position can be estimated. For the results presented in this paper, 50 realisations of  $\mu(r, z)$  are used, which in the calculations lead to an estimate of the normalised standard deviation of the mean value smaller than 1 dB, i.e.

$$10 \log \left[ \frac{\langle p^2 \rangle + \frac{1}{\sqrt{N}} \langle (p^2 - \langle p^2 \rangle)^2 \rangle^{1/2}}{\langle p^2 \rangle} \right] < 1, \quad (10)$$

where  $N = 50$  is the number of realisations and  $p$  the calculated pressure. The mean pressure is calculated for the screened and unscreened cases separately before determining the insertion loss.

### 2.1.3. Approximation of the turbulence representation

The elements of  $M_\mu$  are proportional to  $\mu(r, z)$  and without turbulence all elements of  $M_\mu$  are equal to zero. The matrix  $M^-$  would then be factored into a lower and an upper triangular matrix only once and the solution obtained evolutionary via Gaussian elimination. With a non-zero  $M_\mu$  one would need to factorize  $M^- - \frac{1}{2}M_\mu$  for each range step. To avoid this, and thereby decrease the calculation cost by approximately half, an approximation is made:

$$M_\mu \frac{\bar{\phi}(r + \Delta r) + \bar{\phi}(r)}{2} \cong M_\mu \bar{\phi}(r). \quad (11)$$

The error introduced using the above approximation depends on the discretization and the strength of the turbulence and becomes very small at each range step, but accumulates over distance. In the calculations the value  $\mu_0^2 = 3 \cdot 10^{-6}$  of the strength of the turbulence is used, which leads to an acceptable error (e.g. at 500 Hz the error of the mean pressure is about 0.15 dB at range 1000 meters). With the screen, however, the approximation (11) leads to unstable solutions for some realisations at 1000 Hz. Therefore all calculations with a screen at 1000 Hz are made without this approximation.

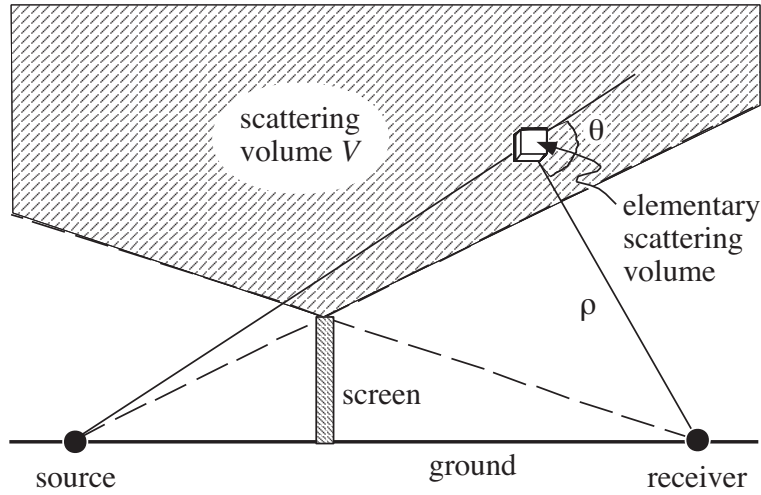


Figure 1. Geometry for the scattering cross-section.

## 2.2. Sound scattering cross-section

Inhomogeneities in the atmosphere will scatter acoustic energy down into the shadow formed by a barrier. One way to estimate the scattered energy is by using the sound scattering cross-section by Tatarskii [2]. This is a single scattering approximation where the turbulence is assumed weak enough so that the wave incident on an inhomogeneity can be approximated by the wave calculated for a non-turbulent atmosphere. Furthermore a far field condition is invoked,

$$\rho \gg l^2/\lambda, \quad (12)$$

where  $\lambda$  is the acoustic wavelength and  $\rho$  the distance from an elementary scattering volume to the receiver (see Figure 1). Condition (12) justifies an uncorrelated summation of the contribution from different elementary scattering volumes and the total received scattered energy can be written as [1]

$$E_s = \int_V p_0^2 \frac{\sigma(\theta)}{\rho^2} dV, \quad (13)$$

where  $p_0$  is the incident pressure,  $\sigma(\theta)$  the scattering cross-section, and  $\theta$  the scattering angle. The volume of integration  $V$  consists of all points in line of sight from both source and receiver (i.e. above both dashed lines in Figure 1). Following Tatarskii [2, p. 160] the scattering cross-section is written

$$\sigma(\theta) = \frac{\pi k_0^4}{2} \cos^2 \theta \left[ \frac{\Phi(\kappa)}{T_0^2} + \frac{4F(\kappa)}{c_0^2} \cos^2 \frac{\theta}{2} \right], \quad (14)$$

where  $\Phi(\kappa)$  and  $F(\kappa)$  are the spectral densities of the temperature and the wind velocity fluctuations respectively,  $T_0$  the mean temperature,  $c_0$  the mean sound

velocity, and  $\kappa$  the wave number of the turbulence, fulfilling the Bragg condition

$$\kappa = 2k \sin \frac{\theta}{2}. \quad (15)$$

The incident pressure  $p_0$  in equation (13) is calculated without taking into account the field diffracted by the screen. This will lead to an overestimation of the scattered energy since the strongest scattering will come from parts of the scattering volume that are near the shadow boundary, where the incident pressure is weakened by diffraction. A more accurate prediction of the scattered energy can be obtained by considering the diffracted field in the entire scattering volume. Equation (13) describes the time average of the energy scattered by turbulence. The turbulence can be seen as a composition of Bragg planes with separation distance  $2\pi/\kappa$  causing scattering of energy proportional to the spectral density at  $\kappa$ .

According to this model the scattered energy will, relative to free field, change with the same factor as the geometry is scaled. To see this let the height of the screen, as well as its distance from source and receiver, be doubled. Substituting for these new variables in the integral (13) will cause an increase by a factor eight in  $dV$  and a factor four in  $\rho^2$ . Relative to free field  $p_0^2$  will stay constant and, as a result, the scattered energy will be doubled (i.e. increased by 3 dB relative to free field).

For a receiver positioned on the surface of the hard ground a pressure doubling is assumed. When the receiver is located above ground, each elementary scattering volume scatters at different angles the direct and ground reflected energy to the receiver. The different scattering angles correspond to different wave numbers of the turbulence which are assumed uncorrelated. Therefore, in the case of a receiver well above ground in relation to the acoustic wavelength and the medium correlation length, the direct and reflected energies are added. Points in the scattering volume straight above the receiver do however have the same angle for the direct and the reflected path, but at these points the scattering cross-section is very small due to the large scattering angle, and the error introduced is negligible compared to the energy scattered at smaller angles.

When calculating the integral (13) numerically, the volume of integration  $V$  is increased until further contribution to the scattered energy is negligible, resulting in a volume from the source to receiver about 100 meters high and 200 meters wide.

To get the same spectral density of the stochastic index of refraction in the PE calculations as for the scattering cross-section, only temperature fluctuations

are considered, since a Gaussian correlation function for the wind velocity in longitudinal direction does not lead to a Gaussian spectral density of  $\mu$  [20, 21]. A Gaussian correlation function for the temperature,

$$C_T(s) \equiv \langle T(\mathbf{R} + \mathbf{s}) T(\mathbf{R}) \rangle = \sigma_T^2 e^{-s^2/l^2}, \quad (16)$$

where  $\sigma_T$  is the standard deviation of the temperature fluctuations, results in three-dimensional space to a Gaussian spectral density,

$$\Phi(\kappa) = \frac{\sigma_T^2 l^3}{8\pi^{3/2}} e^{-\kappa^2 l^2/4}. \quad (17)$$

The standard deviation of the fluctuations in index of refraction  $\mu_0$  is related to  $\sigma_T$  according to:  $\mu_0 = \frac{1}{2}\sigma_T/T_0$ .

### 3. Results

In all calculations with a turbulent atmosphere  $\mu_0^2 = 3 \cdot 10^{-6}$  and  $l = 1.1$  m are used, which is in range of typical measured values. A constant sound speed profile is used (i.e.  $n_d(z) \equiv 1$ ). For the discretization in space using the PE method,  $\Delta r$  and  $\Delta z$  are chosen equal, with a length 0.1 m at 500 Hz and 0.05 m at 1000 Hz, i.e. about one seventh of a wavelength. The calculations at 500 Hz are made for three different geometries, changing the distance from the source to the screen  $r_{sc}$  and the height of the screen  $z_{sc}$ :  $(r_{sc}, z_{sc}) = (100, 10)$ ,  $(200, 20)$  and  $(200, 10)$  m. At 1000 Hz, calculations are made only for the geometry  $(r_{sc}, z_{sc}) = (100, 10)$  m. The calculated insertion loss is shown in Figures 2–9. The two solid lines represent insertion loss in a turbulent atmosphere, calculated according to the two different theories: The PE method, and the model using the scattering cross-section together with diffraction theory (UTD). The two dotted lines represent insertion loss in a homogeneous atmosphere, calculated using the PE method and the UTD respectively. The dashed line represents the scattered energy, calculated using the scattering cross-section alone. The insertion loss is shown at ground level in Figures 2–5 and at the height of the screen edge in Figures 6–9. The results are presented as the sound pressure level calculated in the screened case with the unscreened pressure as the reference (i.e. the negative value of insertion loss).

The attenuating stratum used in the PE starts at height  $z_a = 100$  m, with a thickness  $h_a = 100$  m.

The results from the PE calculations for the insertion loss in a non-turbulent atmosphere compared with the results from using UTD show good agreement for receiver range about two times  $r_{sc}$  and more (Figures 2–9). Since the dominating scattering by turbulence will be produced near the shadow boundary

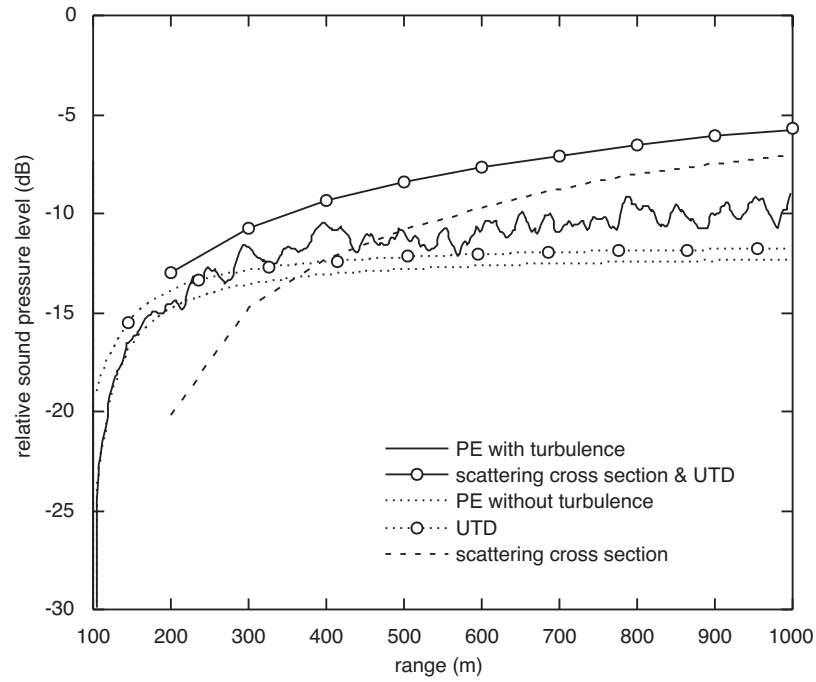


Figure 2. Calculated relative sound pressure level on the ground surface for a 10 m high screen at range 100 m, for the frequency 500 Hz.

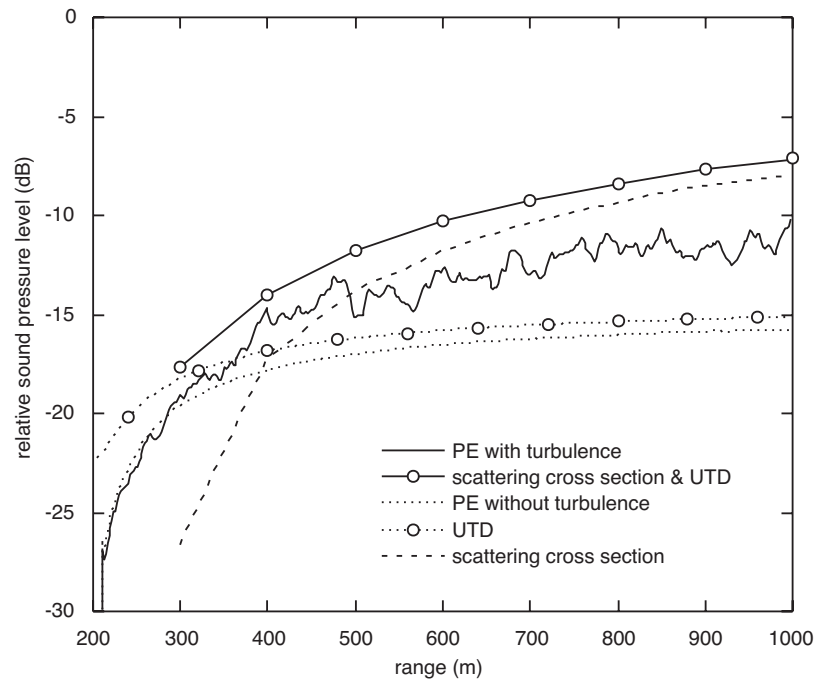


Figure 3. Calculated relative sound pressure level on the ground surface for a 20 m high screen at range 200 m, for the frequency 500 Hz.

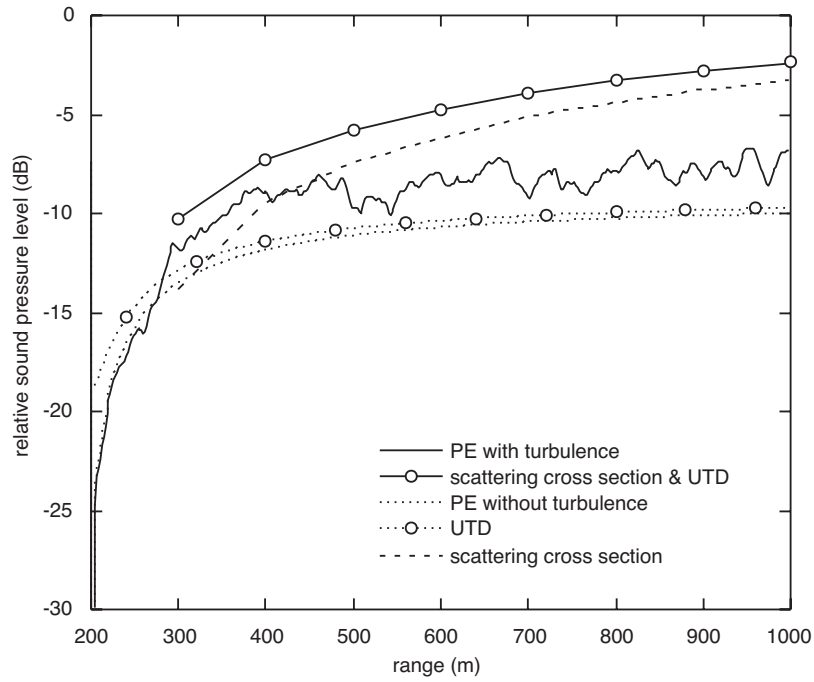


Figure 4. Calculated relative sound pressure level on the ground surface for a 10 m high screen at range 200 m, for the frequency 500 Hz.

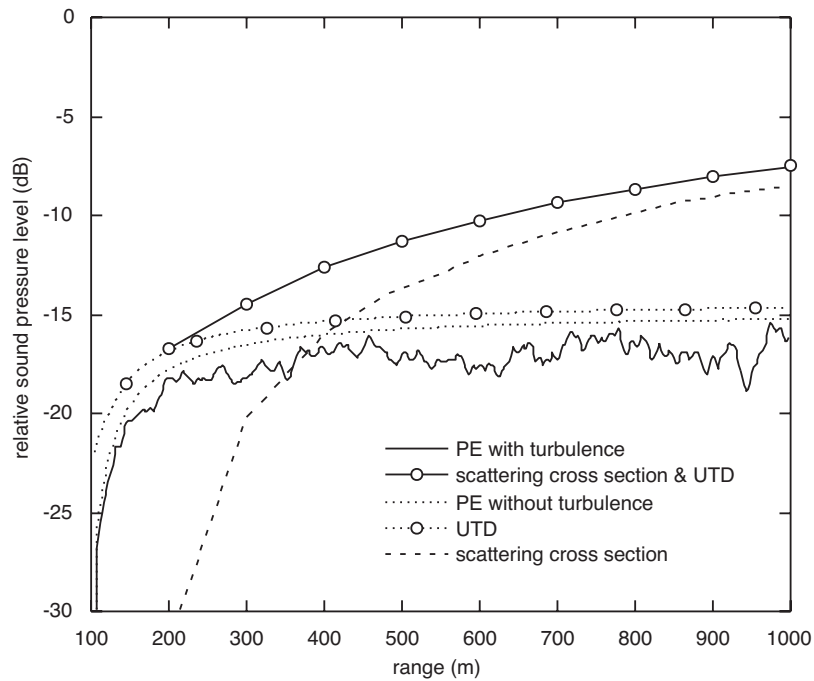


Figure 5. Calculated relative sound pressure level on the ground surface for a 10 m high screen at range 100 m, for the frequency 1000 Hz.

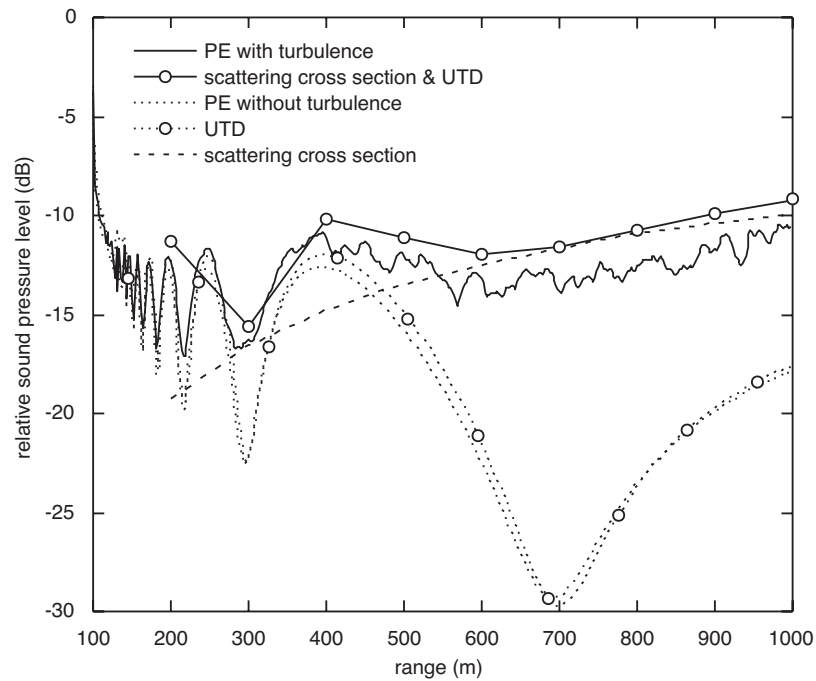


Figure 6. Calculated relative sound pressure level at the height of the screen edge, for a 10 m high screen at range 100 m, for the frequency 500 Hz.

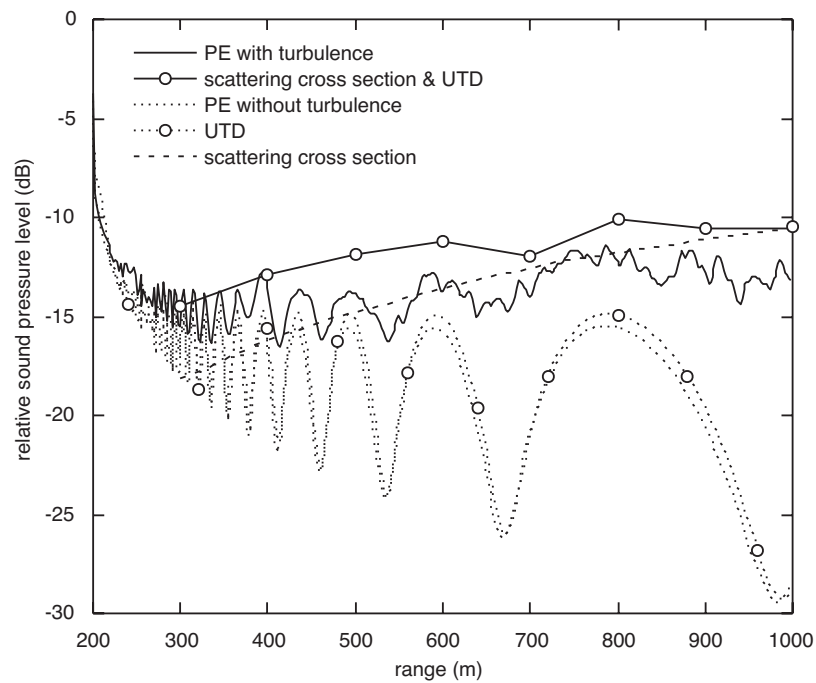


Figure 7. Calculated relative sound pressure level at the height of the screen edge, for a 20 m high screen at range 200 m, for the frequency 500 Hz.

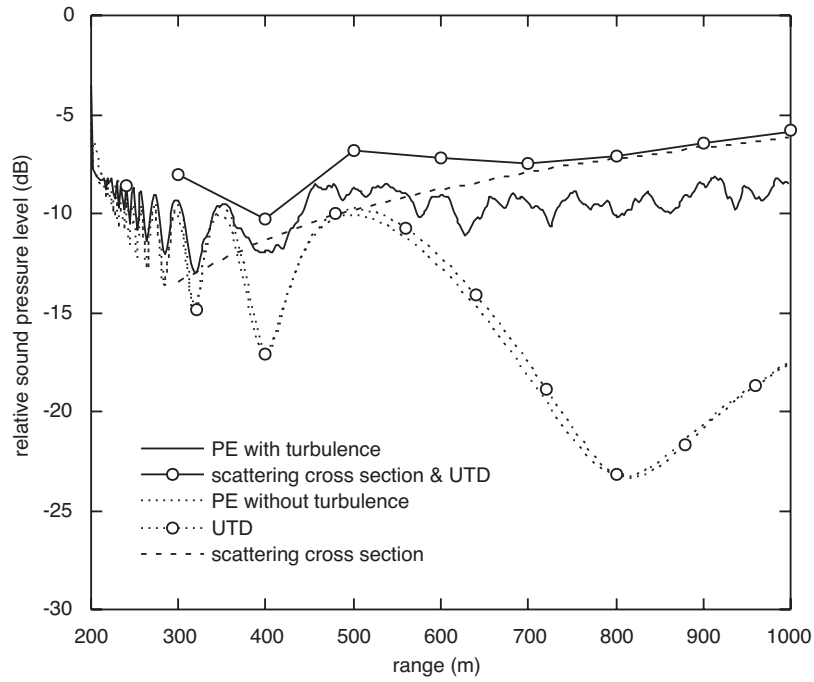


Figure 8. Calculated relative sound pressure level at the height of the screen edge, for a 10 m high screen at range 200 m, for the frequency 500 Hz.

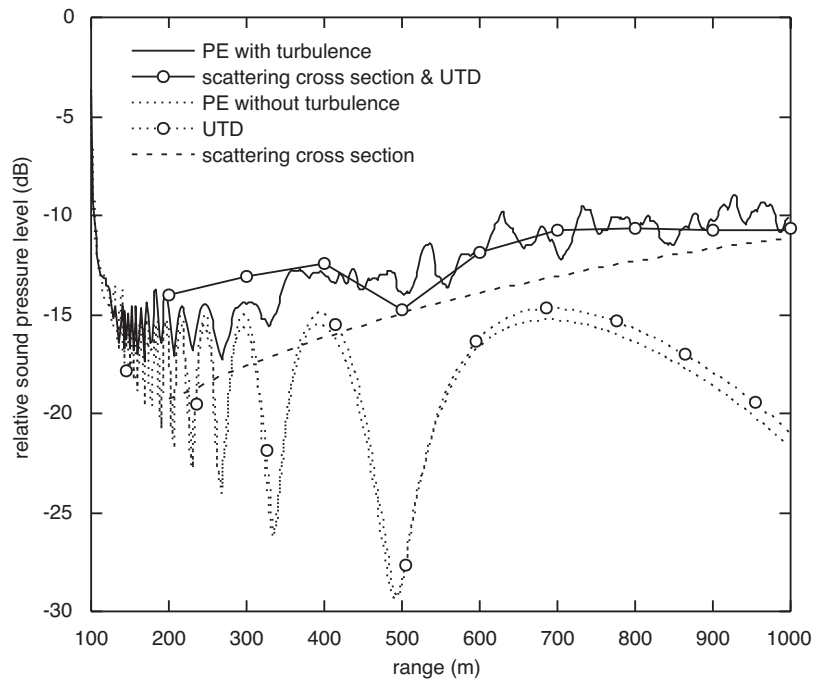


Figure 9. Calculated relative sound pressure level at the height of the screen edge, for a 10 m high screen at range 100 m, for the frequency 1000 Hz.

the PE results for the turbulent atmosphere are expected to be valid from about two times  $r_{sc}$  as well. The implementation of the PE used here is not applicable to geometries where the screen edge is located at a much larger angle than considered here (about  $6^\circ$  at most). This can be seen by comparing the PE results at ground level for  $(r_{sc}, z_{sc}) = (20, 200)$  and  $(10, 200)$  m, for a homogeneous atmosphere (Figures 3 and 4). For the lower screen (Figure 4), the deviation from the predictions by the UTD is smaller than 0.5 dB at longer range; whereas when the screen height is doubled, the deviation is close to 1 dB (Figure 3). By further increasing the screen height, the error in the PE solution will become unacceptable.

Introducing a screen in the PE induces spurious oscillations in the solution. By averaging the solution over a few range steps (corresponding to about one wavelength), these oscillations are diminished [10].

When the receiver is at ground level, the PE calculations show a very small effect of turbulence on insertion loss, as can be seen in Figures 2–5. This is due to constructive interference of the scattered field when the source and receiver are on the surface of a hard ground. It can be described as the hard ground giving rise to a mirror image of each inhomogeneity and the coherency in the turbulence scattering causes the relative sound pressure level to increase over distance in the case without a screen. At 1000 meters range the increase is about 2 dB at 500 Hz and 6 dB at 1000 Hz. In the case with a screen the efficient scattering volume is smaller and has large scattering angles, leading to a weaker image scattering and, therefore, the PE predicts a small decrease in insertion loss at ground level when taking turbulence into account. At 1000 Hz the effect from image scattering even grows strong enough to predict an increased insertion loss with turbulence (Figure 5). However, this effect predicted by the PE would not likely be detected in real situations where the ground is neither perfectly flat nor infinitely hard. The model using the scattering cross-section takes turbulence into account only in the screened case and therefore predicts a strong influence of turbulence on insertion loss at ground level. The effect of image scattering is not present above ground. At heights of 10 and 20 meters the PE calculations show sound pressure levels that, for the unscreened cases, are close to 6 dB relative to free field, for the whole range.

The results of practical interest are for the higher receiver positions where there is negligible influence of image scattering. For these cases the two methods lead to similar results and they show that the effect of turbulence on insertion loss is strong. The scattered energy at the height of the screen edge gives, at longer range, an overall decrease in insertion loss of about 2–5 dB (Figures 6–9). At points of cancellation of direct and reflected diffracted waves, the intro-

duction of turbulence causes decorrelation which, together with the scattering from the insonified region, lead to a further decreased insertion loss. It can be seen that the choice of geometry affects the influence of turbulence. When the height and the range of the screen is doubled (Figures 6 and 7) the influence of turbulence scattering increases because the diffracted field becomes weaker while the scattered field stays about the same at longer range. When the distance from the source to the screen is increased (Figures 6 and 8), both the scattered and the diffracted fields grow stronger at longer range. Increasing the frequency will decrease the strength of the diffracted field and lead to an increased influence of the turbulence (Figures 6 and 9). Moreover, increasing the frequency would normally also lead to stronger scattering, but the Gaussian spectral density of the turbulence, used for these predictions, decays rapidly with increasing wave number and does not yield the expected, increased scattering when the frequency is changed from 500 to 1000 Hz.

For the receiver at the height of the screen edge, the calculations using the PE and the scattering cross-section show good agreement for  $(r_{sc}, z_{sc}) = (100, 10)$  m, both at 500 and 1000 Hz (Figures 6 and 9). However, when the screen is located 200 m from the source, the scattering cross-section predicts about 3 dB stronger scattering than the PE, at longer range (Figures 7 and 8). The reasons for these differences are not clear to the author but are assumed to depend mainly on three things. First, neglecting diffraction when calculating the incident pressure  $p_0$  in equation (13) leads to an overestimation of the scattered energy. Second, the single scattering approximation may be too coarse for these large geometries. Third, there could be large effects from modelling the turbulence as two-dimensional (in the PE method) instead of three-dimensional. Both the limitation of applicability of the single scattering approximation and the effects from modelling the turbulence as two-dimensional should be further investigated.

## 4. Conclusions

The finite difference PE method is applicable to a situation with a screen, as also shown by Salomons [10]. The applicability is however restricted to a screen that is low in comparison to its distance from the source and receiver.

For the situations studied here both the PE method and the model using the scattering cross-section lead to similar results when calculating the energy scattered by turbulence into an acoustic shadow formed by a screen. This indicates that both models are applicable to the situation. There are, however, large differences between the two models, and discrepancies between their results. This calls for further investigation of their accuracy and range of applicability

via comparison of numerical and measured data. In particular, the effects of modelling the atmosphere as two-dimensional and the limitation of the single scattering approximation should be clarified.

The model using the scattering cross-section is not restricted to small angles from the horizontal, as is the PE method, and is much faster numerically. Therefore, in situations where it is applicable it could be an alternative to the PE.

For the situations presented here the scattering by turbulence is shown to significantly decrease the sound reduction by a screen.

When the source is on a hard ground the PE method predicts a strong constructive interference of the turbulence scattering at ground level. The constructive interference is stronger without a screen and therefore the turbulence causes a small decrease in insertion loss at ground level.

An approximation for the inclusion of turbulence in the CN-PE is presented. For the turbulence strength used here, the approximation leads to acceptable errors in all cases without a screen. However, in the case with a screen at 1000 Hz the calculations become unstable. The approximation makes the algorithm approximately twice as fast and, despite the instability caused by the introduction of the screen, can be useful for a variety of applications involving a turbulent atmosphere.

### Acknowledgements

I am very grateful for the nine week visit to the splendid working atmosphere of the Institute for Microstructural Sciences at the National Research Council of Canada. I would like to thank Gilles Daigle for inviting me and for his and Michael Stinson's excellent guidance. I am grateful for many valuable discussions with them and David Havelock. My sincere thanks as well to Professor Vladimir Ostashev for sharing some of his knowledge with me. This work is financially supported by the Swedish Environmental Protection Agency (SNV) and the Swedish Transport and Communications Research Board (KFB).

### References

- [1] Daigle, G. A., Diffraction of sound by a noise barrier in the presence of atmospheric turbulence. *J. Acoust. Soc. Am.*, Vol. 71, 1982, pp. 847-854.
- [2] Tatarskii, V. I., The effects of the turbulent atmosphere on wave propagation. Keter Press, Jerusalem, 1971

- [3] Gilbert, K. E., Raspet, R. and Di, X., Calculation of turbulence effects in an upward-refracting atmosphere. *J. Acoust. Soc. Am.*, Vol. 87, 1990, pp. 2428-2437.
- [4] Gilbert, K. E. and Di, X., A fast Green's function method for one-way sound propagation in the atmosphere. *J. Acoust. Soc. Am.*, Vol. 94, 1993, pp. 2343-2352.
- [5] Raspet, R. and Wu, W., Calculation of average turbulence effects on sound propagation based on the fast field program. *J. Acoust. Soc. Am.*, Vol. 97, 1995, pp. 147-153.
- [6] L'Espérance, A., Herzog, P., Daigle, G. A. and Nicolas, J. R., Heuristic model for outdoor sound propagation based on an extension of the geometrical ray theory in the case of a linear sound speed profile. *Applied Acoustics*, Vol. 37, 1992, pp. 111-139.
- [7] Gilbert, K. E. and White, M. J., Application of the parabolic equation to sound propagation in a refracting atmosphere. *J. Acoust. Soc. Am.*, Vol. 85, 1989, pp. 630-637.
- [8] Attenborough, K., Taherzadeh, S., Bass, H. E., Di, X., Raspet, R., Becker, G. R., Güdesen, A., Chrestman, A., Daigle, G. A., L'Espérance, A., Gabillet, Y., Gilbert, K. E., Li, Y. L. and White, M. J., Naz, P., Noble, J. M. and van Hoof, H. A. J. M., Benchmark cases for outdoor sound propagation models. *J. Acoust. Soc. Am.*, Vol. 97, 1995, pp. 173-191.
- [9] Galindo Arranz, M., The parabolic equation method for outdoor sound propagation. Department of Acoustic Technology, Technical University of Denmark. Doctoral dissertation. Report No. 68, 1996.
- [10] Salomons, E. M., Diffraction by a screen in downward sound propagation: A parabolic-equation approach. *J. Acoust. Soc. Am.*, Vol. 95, 1994, pp. 3109-3117.
- [11] Sack, R. A. and West, M., A parabolic equation for sound propagation in two dimensions over any smooth terrain profile: The generalised terrain parabolic equation (GT-PE). *Applied Acoustics* Vol. 45, 1995, pp. 113-129.
- [12] Stinson, M. R., Havelock, D. I. and Daigle, G. A., Comparison of predicted and measured sound pressure levels within a refractive shadow in the presence of turbulence. *Proc. Inter-Noise 95*, 1995, pp. 327-330.
- [13] Kouyoumjian, R. G. and Pathak, P. H., A uniform geometrical theory of diffraction for an edge in a perfectly conducting surface. *Proc. IEEE* Vol. 62, 1974, pp. 1448-1461.
- [14] Rasmussen, K. B., Model experiments related to outdoor propagation over an earth berm. *J. Acoust. Soc. Am.*, Vol. 96, 1994, pp. 3617-3620.

- [15] Kawai, T., Sound diffraction by a many-sided barrier or pillar. *Journal of Sound and Vibration*, Vol. 79, 1981, pp. 229-242.
- [16] Claerbout, J. F., Fundamentals of geophysical data processing. McGraw-Hill, New York, 1976.
- [17] West, M., Gilbert, K. and Sack, R. A., A tutorial on the parabolic equation (PE) model used for long range sound propagation in the atmosphere. *Applied Acoustics* Vol. 37, 1992, pp. 31-49.
- [18] L'Espérance, A., Nicolas, J. and Daigle, G. A., Insertion loss of absorbent barriers on ground. *J. Acoust. Soc. Am.* Vol. 86, 1989, pp. 1060-1064.
- [19] Stinson, M. R. and Daigle, G. A., Meteorological measurements for use in sound propagation calculations. *Proc. 7th Int. Symp. on Long-Range Sound Propagation*, Lyon, France, 1996, pp. 137-147.
- [20] Mellert, V., Ostashev, V. and Wandelt, R., Sound scattering by scalar and vector random fields. *Proc. 6th Int. Symp. on Long-Range Sound Propagation*, Ottawa, Canada, 1994 pp. 334-347.
- [21] Ostashev, V. E., Sound propagation and scattering in media with random inhomogeneities of sound speed, density and medium velocity. *Waves in Random Media* Vol. 4, 1994, pp. 403-428.